Quantifying river water contributions to riparian trees along a losing river: Lessons from stable isotopes and iteration method

Yue Li[1, 2], Ying Ma[1, 2], Xianfang Song[1, 2], Qian Zhang[3], Lixin Wang[4]

[1]Key Laboratory of Water Cycle and Related Land Surface Processes, Institute of Geographic Sciences and Natural Resources Research, Chinese Academy of Sciences, Beijing 100101, China

[2]University of Chinese Academy of Sciences, Beijing 100049, China

[3]Institute of Geographic Sciences and Natural Resources Research, Chinese Academy of Sciences, Beijing 100101, China

[4]Department of Earth Sciences, Indiana University-Purdue University Indianapolis (IUPUI), Indianapolis, IN 46202, United States

Correspondence to: Ying Ma (maying@igsnrr.ac.cn)

Abstract. River water plays a critical role in riparian plant water use and riparian ecosystem restoration along losing rivers (rivers losing flow into underlying groundwater) under warming climates. How to quantify the contributions of river water to riparian plants under different groundwater levels and the related responses of plant water use efficiency is a great challenge. In this study, observations of water isotopes (δ^2H and $\delta^{18}O$), ^{222}Rn, and leaf $\delta^{13}C$ were conducted for deep-rooted riparian weeping willow (*Salix babylonica* L.) in 2019 (dry year) and 2021 (wet year) along the Chaobai River in Beijing, China. We proposed an iteration method in combination with the MixSIAR model to quantify the proportional river water contribution to transpiration of riparian *S. babylonica* and its correlations with the water table depth and leaf $\delta^{13}C$. Results showed that riparian *S. babylonica* took up deep water (in the 80−170 cm soil layer and groundwater) by 56.5 ± 10.8%. River water that recharged riparian deep water was an indirect water source and contributed by 20.3% of water to riparian trees near the losing river. Significantly increasing river water uptake (by 7.0%) and decreasing leaf $\delta^{13}C$ (by −2.0‰) of riparian trees were observed as the water table depth changed from 2.7 m in dry 2019 to 1.7 m in wet 2021 ($p < 0.05$). The higher water availability probably promoted stomatal opening and thus increasing transpiration water loss, which led to the decreasing leaf $\delta^{13}C$ in wet year compared to dry year. It was found that the river water contribution to riparian *S. babylonica* was negatively correlated with the water table depth and leaf $\delta^{13}C$ in linear functions ($p < 0.001$). The rising groundwater level would trigger riparian trees to increase the water extraction from groundwater/river and show a consumptive river-water-use pattern, which could not be recommended in order to protect both rivers

and riparian vegetation. This study provides critical insights into understanding the mechanisms of water cycle in groundwater-soil-plant-atmosphere continuum, managing water resources and riparian afforestation along losing rivers.

1 Introduction

Ongoing climate warming and groundwater overexploitation have altered river runoff and bank storage globally, further leading to widespread risks of rivers losing flow into underlying groundwater ("losing" river) and even running dry (Winter et al., 1998; Schindler and Donahue, 2006; Allen et al., 2015; Jasechko et al., 2021). Water replenishment to losing rivers and riparian revegetation have been pushed forward worldwide to restore the river ecosystem (Smith et al., 2018; Long et al., 2020). The water replenishment to losing rivers contributed by 40% to bank storage and groundwater storage recovery (Long et al., 2020). However, large-scale riparian revegetation increased plant transpiration substantially, which in turn led to great loss of riparian bank storage and even river runoff (Moore and Owens, 2012; Dzikiti et al., 2013; Missik et al., 2019; Mkunyana et al., 2019). Therefore, determining what water sources and how much river water is taken up by riparian trees and the responses of tree water use characteristics to groundwater level variations can help implement management strategies for maintaining river runoff and tree water need of revegetated riparian zones.

The potential water sources of riparian trees along a losing river are generally considered a mix of soil water at different depths, groundwater, and river water (Alstad et al., 1999; White and Smith, 2020). However, there is a debate on whether river water is a potential water source of riparian trees and how it becomes available to plants. Most of previous studies considered river water as a direct water source to evaluate the river water contribution (RWC) to transpiration of riparian trees (Alstad et al., 1999; Zhou et al., 2017; White and Smith, 2020). These studies showed that river water directly contributed up to 80% to riparian plant transpiration based on the stable isotopic signatures of different water sources and plant stem water (Dawson and Ehleringer, 1991; Busch et al., 1992; Alstad et al., 1999; Zhou et al., 2017; White and Smith, 2020). Nevertheless, some studies argued that river water was not a potential water source and rarely contributed to riparian trees (Dawson and Ehleringer, 1991; Bowling et al., 2017; Wang et al., 2019a). Dawson and Ehleringer (1991) firstly discovered that the mature streamside trees growing in or next to a perennial river did not use river water but depended on water from deeper strata. Similar finding has also been found in riparian phreatophytic trees (*Populus fremontii* and *Salix gooddingii*)

and riparian deep-rooted tree species (Busch et al., 1992; Bowling et al., 2017; Wang et al., 2019a). Even under shallow groundwater with high salinity, no river water was directly taken up by riparian *Eucalyptus coolabah* alongside an ephemeral arid zone river in Australia (Costelloe et al., 2008). Growing evidence showed that riparian trees rarely took up river water directly at a certain distance away from the riverbank because their lateral roots could not reach the river (Mensforth et al., 1994; Thorburn and Walker, 1994); Nevertheless, riparian trees could indirectly utilize river water that recharges deep zone (e.g., deep soil water and groundwater) when their roots tap into the groundwater level (Mensforth et al., 1994; Wang et al., 2019a). If we take river water as a direct water source, the RWC to transpiration of riparian trees may be overestimated. How to separate and quantify the contributions of the indirect river water source to riparian trees near losing rivers is a great challenge.

The graphical inference and direct comparison of stable isotopic values between plant stem water and different water sources (Dawson and Ehleringer, 1991; Busch et al., 1992; Costelloe et al., 2008; Zhao et al., 2016), statistical two- or multi-source linear mixing models (Alstad et al., 1999; Zhou et al., 2017), and the MixSIAR Bayesian mixing model (Wang et al., 2019a; Wang et al., 2020; White and Smith, 2020; Li et al., 2021) integrated with stable isotopes (δ^2H and $\delta^{18}O$) have been widely used to identify the potential water sources taken up by riparian trees. The MixSIAR model has more advantages in quantifying water source contributions and accounting for uncertainties in the isotopic values (Stock and Semmens, 2013; Ma et al., 2016). The RWC to riparian trees can be estimated by quantifying both the direct water source contributions to riparian trees and the RWC to riparian deep water. A multi-iteration method (Marek et al., 1990; Zaid, 2010) is key to calculate the proportional contributions of total (old and current) river water to riparian deep water, which improves the estimation accuracy of the RWC to riparian trees. The radioactive isotope (^{222}Rn) has been widely used for tracing groundwater origins and corresponding pathways in the riparian zone (Close et al., 2014; Zhao et al., 2018). It is helpful to estimate the residence time of recharged groundwater from river water and its effects on the RWC to riparian trees. A combination of these methods can give a more reliable quantification of the RWC to riparian trees.

The RWC to riparian trees could substantially affect the leaf-level water use efficiency (WUE) and growth of riparian trees. Tree WUE is a key characteristic of plant water use, which can be defined as the ratio of photosynthetic rate to transpiration rate. Since leaf $\delta^{13}C$ values are positively related to tree WUE, leaf $\delta^{13}C$ has been widely used as an indicator of tree WUE for C_3 photosynthesis plants (Farquhar et al., 1989). For example, Thorburn and Walker (1994) found that the riparian *Eucalyptus camaldulensis* beside the ephemeral stream had

higher tree WUE with more frequent access to river water based on the leaf $\delta^{13}C$ measurements. Moreover, the fluctuation of the water table depth (WTD) in the riparian zone resulting from changing river water levels plays a critical role in the RWC to riparian trees and tree WUE (Horton and Clark, 2001; Liu et al., 2017; Xia et al., 2018). However, little attention has been paid to quantifying the relationships between the RWC to riparian trees and tree WUE or WTD near a losing river.

The overall aim of this study was to clarify the effects of river water on water use of riparian trees along a gradient of WTD. Focusing on a losing river in Beijing, China, the specific objectives of this study were to: (1) propose an iteration method together with the MixSIAR model and water stable isotopes ($\delta^{2}H$ and $\delta^{18}O$) to quantify the RWC; (2) determine the proportional contributions of river water to riparian trees at different distances away from the riverbank; (3) identify the relationships between the RWC to riparian trees and WUE (indicated by leaf $\delta^{13}C$ values) as well as WTD. These results will provide critical insights into plantation management, bank storage conservation and ecosystem health for losing rivers.

2 Materials and methods

2.1 Study area

The study area was in the reaches of the Chaobai River, located in Shunyi district, Beijing, China (40°07′30″N, 116°40′37″E) (Fig. 1). The temperate continental sub-humid monsoon climate prevails in this area, with an annual mean temperature and evaporation of 11.5 ℃ and 1175 mm, respectively. The average total precipitation from April to November between 1961 and 2021 is 532.8 mm, with 84.5% of which falling in rainy season (from June to September) (Fig. 2a). Due to continuous drought and groundwater overexploitation, the Chaobai River dried up from 1999 to 2007 and the riparian ecosystem seriously degraded. The “ecological water” (including reclaimed water, reservoir water, and diverted water by the South-to-North Water Transfer Project) has been supplied via a systematic water release by dams to restore this dry river since 2007. A total of 51.1 million and 380 million cubic meters of ecological water sources were released to the Chaobai River in 2019 and 2021, respectively. More than 33 km^2 of the riparian zone has been revegetated until 2020. The *Salix babylonica* (L.) was one of the most widely planted species alongside the Chaobai River. Three plots at distances of 5 m (D05), 20 m (D20), and 45 m (D45) away from the riverbank were selected for field measurements and sample collection (Fig. 1).

2.2 Field measurements and data collection

The field measurements were conducted from April to November in 2019 and 2021, with no field observation in 2020 due to the COVID-19. The daily precipitation data from 1961 to 2021 and the daily mean temperature (T), relative air humidity (RH), solar radiation and reference evapotranspiration (ET_0) data during the observation period in the Shunyi district were collected from the China Meteorological Data Service Centre (http://data.cma.cn/en). Daily mean vapour pressure deficit (VPD) was calculated using the RH and T data (Schoppach et al., 2019).

The groundwater levels in each plot were recorded monthly in 2019 and 2021 via a pressure stage gauge (HOH-S-Y, King Water Co Ltd., Beijing, China) installed in the groundwater monitoring well. The river water level was recorded using a water level gauge at the same time with the observation of groundwater levels.

2.3 Sample collection and isotopic analyses

Twelve sampling campaigns on May 5, June 14, July 26, August 15, September 26, November 5 in 2019 and April 24, May 25, June 26, July 15, September 1, November 5 in 2021 were conducted to collect groundwater, river water, soil, stem, and leaf samples. Groundwater in each plot was sampled by a sucking pump from the monitoring well, and a plexiglass hydrophore water sample collector with capacity of 1L was used to collect the nearby river water. Precipitation was sampled after each precipitation event via a device consisting of a funnel, a polyethylene bottle, and a ping-pong ball. A total of 135 precipitation samples were collected throughout the whole years of 2019 and 2021. All precipitation, groundwater, and river water samples were stored in a refrigeration box with several ice bags to minimize evaporation in the field, then they were delivered to the laboratory and kept at 4 ℃ in the refrigerator until water isotope (δ^2H and $\delta^{18}O$) analysis. The groundwater and river water were also collected with 100-ml brown glass vials to measure ^{222}Rn concentration in the field.

One riparian *S. babylonica* tree was chosen in each plot for δ^2H and $\delta^{18}O$ measurements in xylem water as well as $\delta^{13}C$ analysis in plant leaves. The mean diameter at breast height of three sampled trees was 28.6 ± 4.4 cm. Five mature and suberized stem samples were taken from the same riparian *S. babylonica* tree in each plot using an averruncator with the length of 5 m. We removed the bark and phloem of the sampled stems, and then put the remaining xylem samples into a 12-ml brown glass vial sealed with parafilm. Meanwhile, the mature leaves without petioles were sampled from the collected stems using pruning shears. The remaining xylem and mature leaf samples were stored in a refrigeration box with several ice bags in the field. Then the xylem samples were

transported to the laboratory and kept in a refrigerator at −10 ℃ before water extraction and isotope analysis. The mature leaves were oven-dried at 65 °C for 72 h on the day of sampling, then grinded and passed through a 0.15 mm sieve to analyze leaf $\delta^{13}C$ (Wang et al., 2019b; Cao et al., 2020).

Soils at depths of 0−5, 5−10, 10−20, 20−30, 40−60, 60−80, 90−110, 150−170, 190−210, 250−270, and 280−300 cm in one soil profile near the selected *S. babylonica* trees were sampled by a power auger (CHPD78, Christie Engineering Company, Sydney, Australia). One portion of each soil sample was put into a 12-ml brown glass vial and stored at −10 ℃ before water stable isotope analysis, and the other portion was packed into an aluminum box for gravimetric soil water content (SWC) measurement via the oven-drying method (Wang et al., 2019b; Li et al., 2021).

The automatic cryogenic vacuum distillation system (LI-2100, LICA, Beijing, China) was used to extract water from xylem and soil samples, which generally ran for at least 2.5 h. We weighed all the xylem and soil samples before and after extraction. Subsequently, the efficiency of water extraction was calculated in order to ensure the water extraction efficiency above 99% to avoid isotopic fractionation during water extraction. The $\delta^{2}H$ and $\delta^{18}O$ in soil water, river water, groundwater, and precipitation were analyzed through an isotopic ratio infrared spectroscopy system (IRIS) (DLT-100, Los Gatos Research, Mountain View, USA) (Li et al., 2021). The Isotope Ratio Mass Spectrometry system (IRMS) (MAT253, Thermo Fisher Scientific, Bremen, Germany) which could prevent from organic pollution of plants was used to measure $\delta^{2}H$ and $\delta^{18}O$ in xylem water as well as leaf $\delta^{13}C$ value. There was the same measurement accuracy for both the IRIS and IRMS systems (±1‰ for $\delta^{2}H$ and ± 0.1‰ for $\delta^{18}O$). The Vienna Standard Mean Ocean Water (VSMOW) was used to calibrate and normalize the $\delta^{2}H$ and $\delta^{18}O$ measurements in different waters, while the Vienna Pee Dee Belemnite (V-PDB) was used for calibrating leaf $\delta^{13}C$ values.

The ^{222}Rn concentration in the groundwater and river water samples (C_{Water}, Bq/l) was determined based on the air ^{222}Rn concentration values (C_{Air}, Bq/m^3) measured by a ^{222}Rn monitor (Alpha GUARD PQ2000 PRO, Bertin Instruments, Germany). 100 ml of the water sample was slowly poured into the air-tight glass bottles and then purged with air in a closed gas cycling system. The C_{Air} in the ^{222}Rn monitor was recorded at a 10-minute interval. The air inside the measurement set-up had maintained a certain ^{222}Rn concentration right before the water sample injection (C_{System}, Bq/m^3). It is generally assumed that the existing C_{System} can be ignored accordingly when C_{System} is around or lower than 80 Bq/m^3. In this study, more than four intervals were conducted to ensure that the

C_{System} was less than 80 Bq/m^3. The measurement range of C_{Air} was 2–2,000,000 Bq/m^3 with a measurement precision of 3%. The C_{water} can be calculated as:

$$C_{Water}=\frac{C_{Air}\times\left(\frac{V_{System}-V_{Sample}}{V_{Sample}}+k\right)-C_{System}}{1000} \quad (1)$$

where V_{System} is the interior volume of the measuring set-up (ml), which is 1122 ml in this study. V_{Sample} is the volume of water sample (ml). k is the ^{222}Rn distribution coefficient of water/air (–), which can be set as 0.26 within the specified temperature range around a mean room temperature of 20 ℃ (Clever, 1985).

In this study, the average residence time (T_{res}, day) of recharged groundwater from river water was identified based on the ^{222}Rn isotopes (Hoehn and Von Gunten, 1989), which was described as follows:

$$T_{res}=\frac{1}{\lambda}\times\ln\left(\frac{C_e-C_r}{C_e-C_g}\right) \quad (2)$$

where λ represents the decay coefficient (0.181 day^{-1}) (Hoehn and Von Gunten, 1989). C_e represents the ^{222}Rn concentration of background groundwater when the equilibrium between radon production and decay is reached. The measuring ^{222}Rn concentration of groundwater in aquifers more than 100 m away from the riverbank remains constant in this study (with an average value of 7400.0 ± 35.4 Bq/m^3), suggesting that C_e can be defined as 7400.0 Bq/m^3. C_r represents the ^{222}Rn concentration of river water (Bq/m^3); C_g represents the ^{222}Rn concentration of riparian groundwater (Bq/m^3).

2.4 Determination of RWC to riparian trees

In this study, stable water isotopes (δ^2H and δ^{18}O) were integrated within the MixSIAR model and an iteration method was proposed to identify the contributions of the indirect river water that recharged riparian deep water to riparian *S. babylonica* trees (Figs. 4 and 5). Firstly, the direct water source (including soil water in different layers and groundwater) contributions to riparian trees were determined via δ^2H and δ^{18}O in different waters and the MixSIAR model. Secondly, the proportional contributions of river water to riparian deep water (i.e., riparian groundwater and deep soil water in the 80−170 cm layer) were determined by the MixSIAR model and water isotopes. Finally, the proposed iteration method was used to quantify the proportions of the indirect river water source taken up by riparian trees (Figs. 4 and 5).

The MixSIAR model is a Bayesian mixing model which can be integrated with stable isotopes to quantify the proportions of source contributions to a mixture (Stock and Semmens, 2013). The input data of the MixSIAR model include mixture data, source data, and discrimination data. In this study, the mean and standard deviation

(SD) of the isotopic values of each water source for riparian trees/riparian deep water were input as source data into the MixSIAR, while the measured isotopic values of xylem water/riparian deep water were input as raw mixture data into the MixSIAR. The discrimination data for both δ^2H and $\delta^{18}O$ were set to zero, because the input δ^2H and $\delta^{18}O$ values in the MixSIAR were non-fractionated or δ^2H-corrected. The Markov Chain Monte Carlo parameter was set to the run length "very long". Both the trace plots and three diagnostic tests (i.e., Gelman–Rubin, Heidelberger–Welch, and Geweke) were used to determine whether the MixSIAR model converged or not (Stock and Semmens, 2013). Then, the mean and SD values of different water source contributions could be estimated with the MixSIAR model.

2.4.1 Quantifying proportional contributions of direct water sources to riparian trees

Soil water at different depths was taken up by riparian *S. babylonica* directly. We measured soil water isotopes at 11 depths in the three plots. In order to reduce errors in the analytical procedure, four soil layers (0−30 cm, 30−80 cm, 80−170 cm, and 170−300 cm) were used to identify the main root water uptake depth of riparian trees according to seasonal variations in the SWC, water isotopes and WTD. The average soil water isotopes values at depths of 0−5 cm, 5−10 cm, 10−20 cm, and 20−30 cm were calculated for the 0−30 cm soil layer, because the water isotopes went through strong evaporation and SWC varied significantly seasonally. The soil water isotope values at depths of 40−60 cm and 60−80 cm were averaged for the 30-80 cm soil layer, and those values at 90−110 cm and 150−170 cm depths were averaged for the 80−170 cm soil layer since the water isotopes and SWC were relatively stable. The average isotopic values of soil water at deep depths (190−210 cm, 250−270 cm, and 280−300 cm) were calculated for the 170−300 cm soil layer, which varied with the fluctuations of groundwater levels. Groundwater could be regarded as a direct water source for phreatophyte riparian trees (Dawson and Ehleringer, 1991; Busch et al., 1992). As the isotopic composition of soil water in the 170−300 cm layer was similar to that of groundwater, they were considered to be one water source (groundwater). Mensforth et al. (1994) and Thorburn and Walker (1994) characterized the projected edge of canopy as the extension range of lateral roots, which could indicate whether riparian trees take up river water directly or not. In this study, the projected edge of canopy was less than 5 m for riparian *S. babylonica* tree closest to the river (5 m away from the riverbank). It indicated that the lateral roots of *S. babylonica* trees could not tap into the river. Therefore, river water was not considered as a direct potential water source for tree water uptake, while groundwater and soil water in the 0−30, 30−80, and

80−170 cm layers were used as direct potential water sources for riparian *S. babylonica*.

In this study, the δ^2H offsets between the xylem water in riparian trees and its corresponding potential source waters were observed, which could result from δ^2H fractionation in the plant water use processes (Li et al., 2021; Cernusak et al., 2022). These δ^2H offsets could lead to large errors in estimating the water source contributions using the MixSAIR model. In order to eliminate the δ^2H offsets of xylem water from its potential water sources, the measured xylem water δ^2H values were corrected via the potential water source line (PWL) proposed by Li et al. (2021). The PW-excess (PW-excess = $\delta^2H - a_p\delta^{18}O - b_p$; a_p and b_p were slope and intercept of the PWL, respectively) was calculated to indicate the δ^2H deviation from the PWL, which was subsequently subtracted from the measured xylem water δ^2H values. The corrected δ^2H and raw $\delta^{18}O$ in xylem water were set as the mixture data in the MixSIAR model to quantify the contributions of direct water sources to riparian *S. babylonica*.

2.4.2 Quantifying water source contributions to deep soil water and groundwater

The MixSIAR model in conjunction with water isotopes (δ^2H and $\delta^{18}O$) were used to quantify the proportional contributions of current (between previous sampling time t-1 and current sampling time t) river water to riparian deep water (i.e., deep soil water in the 80−170 cm layer or groundwater). The potential water sources of riparian deep soil water in the 80−170 cm layer at t included the in-situ (i.e., water that is already in the deep soil layer or groundwater) soil water in this layer at t-1, soil water in the 0−80 cm layer at t-1, river water between t-1 and t, precipitation between t-1 and t, and groundwater between t-1 and t (Fig. 4a). The potential water sources for riparian groundwater at t were considered as the in-situ groundwater at t-1, soil water in the 0−170 cm layer at t-1, river water between t-1 and t, and precipitation between t-1 and t (Fig. 4b). The δ^2H and $\delta^{18}O$ values in riparian deep water at t were set as the mixture data in the MixSIAR model, while the water isotopes of their potential water sources were considered as the source data.

2.4.3 An iteration method to determine RWC to riparian trees

The proportional contributions of the river water between t-1 and t to riparian trees could be quantified when riparian deep-water contributions to trees and the RWC to riparian deep water were both determined. It was worth noting that riparian deep soil water (80-170 cm) and groundwater can be recharged by river water continuously when the groundwater levels lied below the riverbeds (i.e., losing rivers). Therefore, the proportional contribution of the old river water (before t-1) to riparian deep water should not be ignored. The total RWC to riparian deep

water should be quantified explicitly during the entire period of the river losing flow to riparian deep zone since 2007. We assumed that the contributions of old river water to riparian in-situ deep water were identical to those contributions of current river water (between t-1 and t) to riparian in-situ deep water. An iteration method was proposed to quantify the total RWC to riparian *S. babylonica* trees near the losing rivers, which was described as follows:

$$\begin{aligned} RWC &= P_s * S_r + P_g * G_r \\ &= P_s*(s_r^t + s_r^{t-1}) + P_g*(g_r^t + g_r^{t-1}) \\ &= P_s*(s_r^t + s_r^t*s_s^{t-1} + s_r^t*(s_s^{t-1})^2 + s_g^t*g_r^t + s_g*g_r^t*g_g^{t-1} + s_g^t*g_r^t*(g_g^{t-1})^2) + P_g*(g_r^t + g_r^t*g_g^{t-1} + g_r^t*(g_g^{t-1})^2) \\ &= (P_s*s_r^t + P_g*g_r^t + P_s*s_g^t*g_r^t) + (P_s*s_r^t*s_s^{t-1} + P_g*g_r^t*g_g^{t-1} + P_s*g_r^t*s_g^t*g_g^{t-1}) + (P_s*s_r^t*(s_s^{t-1})^2 + P_g*g_r^t*(g_g^{t-1})^2 + \\ &\quad P_s*s_g^t*g_r^t*(g_g^{t-1})^2) \end{aligned} \quad (3)$$

where S_r and G_r represent total RWC to riparian deep soil water in the 80−170 cm layer and groundwater, respectively. The P_s and P_g represent the contributions of riparian deep soil water in the 80−170 cm layer and groundwater to riparian trees, respectively. The s_r^{t-1} and g_r^{t-1} represent the proportional contributions of the old river water (before t-1) to riparian deep soil water in the 80−170 cm layer and groundwater, respectively. The s_s^{t-1}, s_r^t, and s_g^t represent the proportional contributions of in-situ soil water in the 80−170 cm layer at t-1, river water during t-1 to t, and groundwater during t-1 to t for riparian deep soil water in the 80−170 cm layer at t, respectively. The g_g^{t-1} and g_r^t represent the proportional contributions of in-situ groundwater at t-1 and river water from t-1 to t for riparian groundwater at t, respectively. The expression of "$P_s*s_r^t + P_g*g_r^t + P_s*s_g^t*g_r^t$" in Equation (3) was proposed to determine the current river water (between t-1 and t) contributions to riparian trees. The second iteration ($P_s*s_r^t*s_s^{t-1} + P_g*g_r^t*g_g^{t-1} + P_s*g_r^t*s_g^t*g_g^{t-1}$) and the third iteration ($P_s*s_r^t*(s_s^{t-1})^2 + P_g*g_r^t*(g_g^{t-1})^2 + P_s*s_g^t*g_r^t*(g_g^{t-1})^2$) were used to quantify the proportional contributions of old river water that recharged riparian in-situ deep water to trees (Fig. 5). Only three iterations were applied in this study, because the differences between the RWCs in the third iteration and the next iteration were less than 0.1%. Using this proposed iteration method, we estimated the total proportions of old and current river water in the riparian trees.

2.5 Statistical analysis

One-way analysis of variance (ANONA) incorporating with the Kolmogorov-Smirnov, Levene's and post-hoc Tukey's tests ($p < 0.05$) were used to investigate the statistic differences of different variables. The variables included the WTD, SWC, δ^2H and $\delta^{18}O$ in different water sources and xylems, ^{222}Rn concentration of river water

and groundwater, contributions of different water sources to riparian deep water or trees, and leaf $\delta^{13}C$ values in the three plots in 2019 and 2021. The linear regression model was fitted to the whole dataset in both years to get the general relationships between the WTD, leaf $\delta^{13}C$ values and the RWC to riparian trees. The statistical analysis was performed in the Excel (v2016) and SPSS (24.0, Inc., Chicago, IL, USA).

3 Results

3.1 Hydro-meteorological conditions

The observation period in 2021 was wet with a total precipitation of 802.5 mm, which was 1.8 times higher than for the drier year 2019 (445.6 mm) (Fig. 2a). The precipitation amount during rainy season accounted for 75.4% and 97.0% in 2019 and 2021, respectively. The annual mean temperature during the observation period in 2019 and 2021 was 22.4 ℃ and 21.8 ℃, respectively. The daily mean VPD and ET_0 increased during the observation period, reaching a peak in June and May, respectively (Fig. S1). The average daily VPD during the observation period was significantly higher in dry 2019 (1.1 KPa) than in wet 2021 (0.9 KPa) ($p < 0.05$) (Fig. S1a and b). There was a significant difference in the average daily ET_0 from June to September between dry 2019 (5.0 mm/day) and wet 2021 (4.3 mm/day) ($p < 0.05$), but no significant difference was observed during the remaining observation period between the two years ($p > 0.05$) (Fig. S1c and d). No significant difference in the daily mean net radiation during the observation period was found between dry 2019 and wet 2021 ($p > 0.05$) (Fig. S1 c and d).

The river water level fluctuated between 27.9 m and 28.9 m in 2019 and between 27.7 m and 29.3 m in 2021 (Fig. 3). The mean WTD across the three plots was significantly ($p < 0.05$) deeper in 2019 (2.7 ± 0.3 m) than in 2021 (1.7 ± 0.5 m). The WTD increased with increasing distances from the riverbank in both 2019 and 2021 (Fig. 3). The river water continuously recharged the groundwater system (“losing” river) during the observation periods in 2019 and 2021, indicated by a lower groundwater level than the river water level (Fig. 3). Significantly higher SWC was observed in 2021 compared to 2019 ($p < 0.05$) (Fig. S2). The SWC of each soil layer at D45 was significantly lower than at D05 and D20 in 2021 ($p < 0.05$), while no pronounced difference in the SWC in the 0−30 cm layer was observed among the three plots in 2019 ($p > 0.05$) (Fig. S2).

3.2 Direct water source contributions to riparian trees

Precipitation was significantly more depleted in δ^2H and $\delta^{18}O$ in 2021 (−52.9‰ ± 30.2‰ for δ^2H and −8.1‰ ± 3.8‰ for $\delta^{18}O$) than in 2019 (−29.2‰ ± 18.8‰ for δ^2H and −4.1‰ ± 3.0‰ for $\delta^{18}O$) ($p < 0.05$) (Fig. 6). The slope of the local meteoric water line in 2021 (7.8) was significantly higher than in 2019 (5.5) ($p < 0.05$), which suggested that the falling raindrops undergone stronger sub-cloud evaporation in 2019 (Zhao et al., 2019). The δ^2H and $\delta^{18}O$ in the surface soil water (above 30 cm depth) were significantly lower and more variable in 2021 than in 2019 ($p < 0.05$) (Fig. 6). In contrast, there were slightly higher water isotopic compositions in the 30−170 cm soil layer in 2021 compared to 2019. No significant difference in the isotopic compositions of the soil water below 170 cm depth and groundwater were observed between 2019 and 2021 ($p > 0.05$). The δ^2H and $\delta^{18}O$ in soil water in the 80−170 cm layer were significantly lower than groundwater in 2019 ($p < 0.05$), while no significant difference was observed between soil water isotopes in the 80−170 cm layer and groundwater isotopes in 2021 ($p > 0.05$). Groundwater was significantly more depleted in δ^2H and $\delta^{18}O$ compared to river water in both two years ($p < 0.05$) (Fig. 6). The δ^2H and $\delta^{18}O$ in xylem water during the observation periods in 2019 and 2021 were not significantly different ($p > 0.05$), but they were gradually lower with the increasing distance from the riverbank.

The contributions of the surface soil water to transpiration of riparian trees in 2019 (20.1% ± 9.7%) were similar to 2021 (19.0% ± 10.5%). No significant difference in the soil water contributions to riparian *S. babylonica* was also observed in the 30−80 cm layer between the two years ($p>0.05$) (Fig. 7). The *S. babylonica* tree species principally relied on riparian deep water below the 80 cm depth in both 2019 (55.9%) and 2021 (57.1%). There was no significant difference in the riparian deep-water contributions to transpiration of *S. babylonica* trees between the three distances from the riverbank ($p > 0.05$) (Fig. 7). Nevertheless, the soil water contributions in the 80−170 cm layer to riparian trees decreased with increasing distance from the riverbank in both years, whereas the proportions of groundwater taken up by riparian trees increased from D05 to D45 in both 2019 (from 27.6% to 32.1%) and 2021 (from 17.0% to 32.2%) (Fig. 7). It was found that the groundwater contributions to riparian *S. babylonica* trees increased significantly ($p < 0.05$) from April to July. They plummeted significantly ($p < 0.05$) and reached minimum in September in 2021.

3.3 Water source contributions to riparian deep soil water and groundwater

The primary water sources of riparian deep soil water in the 80-170 cm layer were the in-situ soil water in this layer (mean of 33.1%) and groundwater capillary rise (mean of 25.3%) in 2019 (Fig. 8). In comparison, the in-

situ soil water in the 80-170 cm layer (mean of 23.9%), groundwater capillary rise (mean of 24.6%), and river water (mean of 24.4%) contributed evenly to riparian deep soil water in 2021. The in-situ soil water contribution to riparian deep soil water was significantly higher in 2019 than in 2021 ($p < 0.05$). However, the river water contributed less to riparian deep soil water in 2019 (mean of 15.7%) compared to 2021 ($p < 0.05$). The RWC to riparian deep soil water was the lowest in August in 2019 (11.3% ± 4.5%) and in June in 2021 (13.6 ± 3.8%), respectively. The in-situ soil water contributions to riparian deep soil water showed a significant increase with increasing distance from the riverbank, while the RWC to riparian deep soil water decreased from D05 to D45 in both years ($p < 0.05$) (Fig. 8).

The in-situ groundwater contribution was significantly higher in 2019 (mean of 56.0% ± 11.2%) than in 2021 (37.1% ± 16.7%) ($p < 0.05$) (Fig. 9). The average contribution of the river water to riparian groundwater was 28.1% ± 12.1% during the observation period. There was a significantly higher RWC to riparian groundwater in 2021 (mean of 35.1% ± 11.9%) than in 2019 (mean of 21.1% ± 7.2%) ($p < 0.05$). The lowest RWC (13.0% ± 1.2%) showed in August with the lowest groundwater level of 3.1 m in 2019, whereas river water contributed the highest (47.1% ± 13.2%) to riparian groundwater in July with a higher groundwater level of 1.8 m in 2021 (Figs. 3 and 9). The proportional contribution of the in-situ groundwater for riparian groundwater increased with the increasing distance from the riverbank during the observation periods, while the RWC to riparian groundwater decreased significantly from D05 to D45 ($p < 0.05$) (Fig. 9). There was a significant increase of ^{222}Rn activity in groundwater from D05 (610.1 ± 107.5 Bq/m^3) to D45 (787.4 ± 153.2 Bq/m^3) ($p < 0.05$) (Table 1). The T_{res} of recharged groundwater from river water increased from D05 (0 days) to D45 (0.15 ± 0.13 days) (Table 1). These also indicated that the river recharged riparian deep strata rapidly and frequently, particularly more significant in the plots closer to the riverbank.

3.4 Seasonal variations in RWC to riparian trees

The proportional contributions of river water to riparian *S. babylonica* trees were significantly higher in 2021 (mean of 23.8% ± 7.8%) than in 2019 (mean of 16.8% ± 4.7%) ($p < 0.05$). Specifically, the most significantly monthly difference in the RWC to riparian *S. babylonica* trees between dry 2019 and wet 2021 was up to 19.8% ($p < 0.001$). The monthly maximum RWC to *S. babylonica* trees was significantly higher in wet 2021 (35.2% ± 7.0%) compared to dry 2019 (24.2% ± 3.0%) ($p < 0.05$).

The riparian *S. babylonica* took up the most river water in July (35.2 ± 7.0%) in 2021, whereas the highest

RWC to riparian trees occurred in June (24.2% ± 1.6%) in 2019. The minimum river water uptake for riparian *S. babylonica* in 2021 was in September (17.7% ± 2.7%), while trees took up the least river water in August 2019 (13.2% ± 1.9%). Although the precipitation amount in rainy season was much higher than in drought season ($p <$ 0.001), no significant difference in the RWC to riparian *S. babylonica* trees was observed between the rainy and drought seasons in a same year ($p > 0.05$) (Figs. 2 and 9). The difference values of the RWC to riparian trees between the rainy and dry seasons were not significantly different ($p > 0.05$) in both 2019 (−4.0%) and 2021 (−4.4%) (Fig. 9). These showed that there were no significant seasonal variations in the RWC to riparian trees within a year ($p > 0.05$).

The water uptake of river water by riparian *S. babylonica* was significantly different between the three plots in 2019 ($p < 0.05$), while no difference was observed between the three plots in 2021 ($p > 0.05$) (Fig. 10). Specifically, the RWC to riparian trees decreased significantly by 6.9% from D05 (20.0%) to D45 (13.1%) in 2019 ($p < 0.05$), whereas there was no significant difference in 2021 ($p > 0.05$) (Fig. 10).

3.5 Relationships between leaf $\delta^{13}C$, RWC to riparian trees and WTD

The leaf $\delta^{13}C$ of riparian *S. babylonica* trees was significantly higher in 2019 (−27.7‰ ± 1.0 ‰) than in 2021 (−29.7‰ ± 0.7 ‰) ($p < 0.05$) (Table 2). There was a significant increase of the leaf $\delta^{13}C$ from D05 (−28.8‰) to D45 (−27.0‰) in 2019 ($p < 0.05$), while no significant difference in the leaf $\delta^{13}C$ was observed between the different distances in 2021 ($p > 0.05$). The lowest leaf $\delta^{13}C$ value of riparian trees occurred on August 15 in 2019 and July 14 in 2021, before intense rainfall occurred in both years.

There was a significantly negative relationship between the RWC to riparian trees and WTD ($R^2 = 0.57$; $p <$ 0.001) (Fig. 11a). The leaf $\delta^{13}C$ of riparian *S. babylonica* was found to be negatively correlated with the RWC to riparian trees ($R^2 = 0.61$; $p < 0.001$) but positively related to WTD ($R^2 = 0.37$; $p < 0.001$) in linear functions (Fig. 11b and c). These indicated that deeper WTD (2.7 ± 0.3 m) resulted in lower RWC to riparian *S. babylonica* and higher leaf-level WUE in the drier year 2019. In comparison, the riparian *S. babylonica* under relatively shallower WTD (1.7 ± 0.5 m) led to higher RWC but lower leaf-level WUE in 2021.

4 Discussion

4.1 Advantages and limitations of MixSIAR model and the iteration method

The iteration method in combination with the MixSIAR model and stable water isotopes is particularly useful for

separating and quantifying the proportional contributions of river water to transpiration of riparian trees near a losing river. This integration of methods is more accurate than previous studies (Alstad et al., 1999; Zhou et al., 2017; White and Smith, 2020), which only considered river water as a direct water source of riparian trees without considering their distances from the riverbank and extents of the lateral roots. The primary advantage of the combined method is that it explicitly identifies the direct and indirect water sources of riparian trees according to the distance from the riverbank, the extents of lateral roots, and the process of river recharging riparian deep water. Both the trace plots and three diagnostic tests (i.e., Gelman–Rubin, Heidelberger–Welch, and Geweke) were used to ensure that the MixSAIR model has converged (Stock and Semmens, 2013). Moreover, the MixSIAR model has explicitly considered the uncertainties in the isotopic values and the estimates of source contributions compared to the simpler linear mixing models (Stock and Semmens, 2013; Ma et al., 2016). The strength of the newly proposed multi-iteration method is that it can determine the total contributions of the indirect river water source to riparian trees. The multi-iteration will not stop until there is no significant difference between the results of the last two iterations, which reduces the calculation errors of the RWC to riparian trees.

However, the riparian deep-water sources were identified using the water isotopic data collected between two campaigns (an interval of about one month). The riparian soil water movement was complex, and the water isotopes might not be uniform between two campaigns along the losing river. Assuming the isotopic uniformity over such a time interval may cause uncertainties in estimating the RWC to riparian deep water. In addition, we assumed that the contributions of old river water (before initial time (t-1)) to riparian in-situ deep water were identical with those contributions of current river water (during the observation period between t-1 and t) to riparian in-situ deep water in this study. This could induce some uncertainties on the estimations of the RWC to riparian deep water and the RWC to riparian trees. To minimize this issue, water samples need to be collected more frequently to quantify the contributions of river water to riparian deep water and trees.

4.2 RWC to riparian trees and effects of the distance from the river on RWC

In this study, deep-rooted riparian trees near the losing river were identified to use a small proportion of river water (less than 25%) for transpiration (Fig. 10). The small RWC to riparian trees may be caused by three non-exclusive processes: firstly, the lateral roots of riparian trees further than 5 m away from the riverbank rarely took up river water directly when their projected edges of canopy (less than 5 m in our study) were out of reach of the river (Busch et al., 1992; Thorburn and Walker, 1994). Instead, they took up riparian deep soil water/groundwater

recharged by river water, which likely restricted the RWC to transpiration of riparian trees. Secondly, the ecohydrological separation (Brooks et al., 2010; Evaristo et al., 2015; Allen et al., 2019; Sprenger et al., 2019) might result in large isotopic discrepancies between fast-moving water flow and immobile water for plant water uptake. Although the residence time of recharged groundwater from river water was extremely short (less than 0.28 days) (Table 1), only one third of riparian groundwater was replaced by the lateral seepage of river water (Fig. 9). This probably indicated that river water recharged mobile groundwater quickly but could not completely replace water held tightly in the soil pores (Brooks et al., 2010; Evaristo et al., 2015; Allen et al., 2019). It was consistent with Sprenger et al. (2019) who found that the lateral seepage of river water or rising groundwater level could briefly saturate riparian soils but not entirely replace/flush immobile waters or isotopically homogenize different water pools. Thirdly, several recent studies showed that even phreatophytic/deep-rooted trees predominantly extended roots into fine pores to take up immobile soil water (Evaristo et al., 2015; Maxwell and Condon, 2016; Evaristo et al., 2019). As mentioned above, the immobile water could not be completely replaced by infiltrating river water, which eventually resulted in a small contribution of river water to deep-rooted riparian trees. This ecohydrological separation perspective that plant accessible water pools were separated from the fast-moving water can also be supported by the findings that no significant difference in RWCs to riparian trees between rainy and drought seasons was observed in both dry and wet years (Fig. 9). Because riparian *S. babylonica* trees preferred to rely on immobile water in fine soil pores and they would not change the river water uptake patterns when the fast-moving precipitation input increased (Brooks et al., 2010; Sprenger et al., 2019).

In contrast, Alstad et al. (1999) found that riparian *Salix* trees near a losing river on the northeast side of the Rocky Mountain National Park, Colorado relied on rivers for approximately 80% of its transpiration. It is probably due to the fact that only river water and precipitation were considered as potential water sources for riparian *Salix* in their study. The RWC to riparian *Salix* trees calculated by Alstad et al. (1999) could be overestimated because it likely included all proportions of the indirect river water, in-situ soil water and in-situ groundwater contributions to riparian *Salix* trees. In fact, river water seeped into the saturated/vadose zone across the riparian riverbank and it was taken up by riparian trees indirectly in the form of river-recharged deep soil water/groundwater. In our study, we separated the contributions of indirect river water source (i.e., river-recharged deep soil water in the 80−170 cm layer and groundwater) for riparian trees. The accurate quantification of the indirect RWC to deep-rooted riparian trees could help to determine the effect of riparian plant water use on river runoff along a losing river.

We observed substantially variations in the RWC to riparian trees at interannual (between two years) and spatial (between three distances from the riverbank) scales (Fig. 10). The RWC to riparian *S. babylonica* trees in wet 2021 was 1.4 times higher on average than in dry 2019 (Fig. 10). This is mainly because that the higher groundwater level in wet year induced higher RWC to riparian deep water, while riparian *S. babylonica* trees presented similar root architecture (i.e., phreatophyte) associated with similar water source proportions between dry and wet years (Fig. 10). Thus, the indirect RWC to riparian phreatophyte trees in wet year was higher than in dry year. Although there was no significant difference in the deep water (below the 80 cm layer) contributions to riparian trees between three plots, we observed substantial effect of the declining groundwater level with increasing distance from the riverbank on the decreased indirect RWC to riparian trees in dry 2019 (Fig. 10). Therefore, the interannual and spatial variabilities of the RWC to riparian *S. babylonica* trees were generally attributed to the various RWCs to riparian deep water rather than the water use patterns of riparian trees. Our result is in contrasts to a previous study by Qian et al. (2017) who reported a significant increase of the RWC to *G. biloba* trees in response to the groundwater level decline. This discrepancy was ascribed to the fact that riparian *G. biloba* had a dimorphic root system and shifted their main water sources from shallow soil layer to deeper soil layer. Nevertheless, the potential root growth rate of riparian phreatophyte *S. babylonica* trees can reach 1-13 mm/day, which allows the riparian *S. babylonica* trees to remain in contact with a rising/declining groundwater level and maintain constant water uptake proportions from deep strata below the 80 cm depth (Naumburg et al., 2005).

4.3 Link between RWC/WUE/WTD and the implications

The water uptake patterns of riparian *S. babylonica* trees generally followed the characteristics of a phreatophyte. We observed that leaf WUE of all *S. babylonica* trees across three plots in both dry and wet years were negatively correlated with the indirect RWC to riparian trees and positively related to WTD (Figs. 10, 11b, and 11c). These relationships are consistent with previous studies (Cao et al., 2020; Ding et al., 2020; Behzad et al., 2022). Higher leaf WUE associated with lower RWC to riparian trees and lower groundwater levels are likely because water stress restricts the stomatal conductance and further reduces transpiration rate of riparian trees. Specifically, dry 2019 was characterized as higher water demand (indicated by higher VPD) and lower water availability compared to wet 2021, but the energy resource (indicated by net radiation) for riparian trees was similar between two years (Figs. S1 and S2). We argued that water limitation rather than energy limitation regulated the leaf-level stomatal

conductance of riparian *S. babylonica* trees. The high water demands but low river water availability in dry year probably resulted in stomatal closure of riparian trees to minimize water loss, which could eventually lead to a decrease of transpiration rate and even photosynthetic rate (Fabiani et al., 2021; Behzad et al., 2022). Aguilos et al. (2018) further found that water stress would enhance radiation-normalized WUE because the lack of water availability induced stronger reduction in transpiration than photosynthesis. With no difference in the average net radiation between dry and wet years, the lower river water availability in the dry year probably resulted in an increase of leaf WUE. It can be inferred that riparian *S. babylonica* trees took up more river water and probably showed a consumptive river-water-use pattern in the wet year compared to the dry year. This agreed well with previous studies that the woody plants showed lower leaf WUE and consumptive water-use patterns in rainy season, while they showed higher leaf WUE and conservative water-use patterns with lower soil water availability in dry season (Horton and Clark, 2001; Cao et al., 2020; Behzad et al., 2022). However, consumptive river water taken up by riparian trees could result in a great loss of river water, which should be avoided in the riparian zone of a losing river restored by "ecological water".

The WTD played a critical role in the river water uptake of riparian trees near a losing river (Mensforth et al., 1994; Horton and Clark, 2001; Qian et al., 2017; Zhou et al., 2017). We observed that the proportional contributions of the river water source to riparian trees decreased linearly in response to groundwater level decline, leading to a proportional increase in leaf WUE (Fig. 11a and b). It was consistent with Horton and Clark (2001) who found an exponential increase of the leaf WUE of riparian *Salix gooddingii* with increasing WTD. As mentioned above, we emphasized the key role of reduced water availability on decreasing transpiration rate thus enhancing leaf WUE in this study. Nevertheless, there were some controversial views that leaf WUE of plant species increased firstly and then decreased with increasing WTD (Antunes et al., 2018; Xia et al., 2018). This could be due to the fact that riparian trees could tolerate reduced water availability only within a species-specific threshold, beyond which xylem cavitation and even crown mortality occurs (Naumburg et al., 2005). These indicated that optimal WTD for plant species was related to the highest leaf WUE, under that condition plant species could consume less water for transpiration to maximize CO_2 assimilation (Antunes et al., 2018; Xia et al., 2018). The break point of WTD was not observed in this study (Fig. 11a and b). Further investigations need to be conducted under deeper groundwater levels (WTD > 4 m) to optimize the WTD and riparian plant-water relations.

Our results have important implications for untangling the trade-offs between riparian tree water use and

river runoff management. The proportion of the RWC to riparian trees has been compared between dry and wet years to investigate the effects of river water availability on the water use characteristics of riparian trees. The riparian *S. babylonica* trees showed the highest WUE and the lowest river water uptake proportion under the lowest groundwater level condition (with the WTD of 4 m). The rising groundwater level would trigger riparian trees to show a consumptive river-water-use pattern, which should not be recommended in the revegetated riparian zone beside an ecological-water-recharged losing river. Therefore, the relationships between the RWC to riparian trees, leaf-level physiological characteristics (e.g., leaf WUE) and hydro-meteorological conditions are critical to protect the revegetated riparian zones and maintain river runoff sustainability.

5 Conclusions

In this study, we presented a new iteration method together with the MixSIAR model and stable water isotopes (δ^2H and $\delta^{18}O$) to separate and quantify the proportional contributions of river water to riparian *S. babylonica* in dry 2019 and wet 2021 along a losing river in Beijing, China. It was found that the infiltrating river water exchanged with riparian mobile water quickly but not completely mixing with waters held tightly in the fine pores. Riparian trees near a losing river generally extended roots into fine pores to access the immobile water sources. The isotopic discrepancies between the fast-moving water flow and the immobile water taken up by the roots led to a small RWC (20.3%) to transpiration of riparian trees. The water deficit in the dry year probably induced stomatal closure and larger reduction in transpiration compared to the photosynthesis of riparian trees, thus leading to an evident increase of WUE than in the wet year. The leaf WUE showed a negative correlation with the RWC to riparian trees but was positively related to WTD in linear functions ($p < 0.001$). Riparian *S. babylonica* trees maintained the highest WUE and the lowest river water uptake proportion under deep groundwater condition (with the WTD of 4 m) in this study. These suggested that rising groundwater level triggered riparian trees to increase the river water uptake and show a consumptive river-water-use pattern, which should not be recommended for the water resource management of a losing river restored by ecological water. This study provides valuable insights into riparian afforestation related to water use and ecosystem health.

Data availability: The data that support the findings of this study are available from the corresponding author upon request.

Author contributions: YL: Investigation, Methodology, Formal analysis, Writing - original draft, Writing - review & editing; YM: Methodology, Formal analysis, Conceptualization, Writing - review & editing; XFS: Supervision, Writing - review & editing, Project administration; QZ: Methodology. LXW: Writing - review & editing.

Competing interests: The authors declare that they have no conflict of interest.

Acknowledgements: This work was supported by the National Natural Science Foundation of China (41730749) and the National Key R&D Program of China (2021YFC3201203). Sincere thanks go to Xue Zhang, Yiran Li, Lihu Yang and Binghua Li for their assistance in experiments.

Reference

Allen, C. D., Breshears, D. D., and McDowell, N. G.: On underestimation of global vulnerability to tree mortality and forest die-off from hotter drought in the Anthropocene. Ecosphere. 6, doi:10.1890/ES15-00203.1, 2015.

Allen, S. T., Kirchner, J. W., Braun, S., Siegwolf, R. T. W., and Goldsmith, G. R.: Seasonal origins of soil water used by trees. Hydrology and Earth System Sciences. 23, 1199-1210, 2019.

Alstad, K. P., Welker, J. M., Williams, S. A., and Trlica, M. J.: Carbon and water relations of *Salix monticola* in response to winter browsing and changes in surface water hydrology: an isotopic study using delta C-13 and delta O-18. Oecologia. 120, 375-385, 1999.

Aguilos, M., Stahl C., Burban, B., Hérault B., Courtois, E., Coste, S., Wagner, F., Ziegler, C., Takagi, K. and Bonal, D.: Interannual and seasonal variations in ecosystem transpiration and water use efficiency in a tropical rainforest. Forests. 10(1), 14, 2019.

Antunes, C., Barradas, M. C. D., Zunzunegui, M., Vieira, S., Pereira, A., Anjos, A., Correia, O., Pereira, M. J., and Maguas, C.: Contrasting plant water-use responses to groundwater depth in coastal dune ecosystems.

Functional Ecology. 32, 1931-1943, 2018.

Behzad, H. M., Arif, M., Duan, S., Kavousi, A., Cao, M., Liu, J. and Jiang, Y. Seasonal variations in water uptake and transpiration for plants in a karst critical zone in China. Science of The Total Environment. 160424, 2022.

Bowling, D. R., Schulze, E. S., and Hall, S. J.: Revisiting streamside trees that do not use stream water: can the two water worlds hypothesis and snowpack isotopic effects explain a missing water source? Ecohydrology. 10, 1-12, doi:10.1002/eco.1771, 2017.

Brooks, J. R., Barnard, H. R., Coulombe, R., and McDonnell, J. J.: Ecohydrologic separation of water between trees and streams in a Mediterranean climate. Nature Geoscience. 3, 100-104, 2010.

Busch, D. E., Ingraham, N. L., and Smith, S. D.: Water uptake in woody riparian phreatophytes of the Southwestern United States: A stable isotope study. Ecological Applications. 2, 450-459, 1992.

Cao, M., Wu, C., Liu, J. C., and Jiang, Y. J.: Increasing leaf $\delta^{13}C$ values of woody plants in response to water stress induced by tunnel excavation in a karst trough valley: Implication for improving water-use efficiency. Journal of Hydrology. 586, 124895, doi:10.1016/j.jhydrol.2020.124895, 2020.

Cernusak, L.A., Barbeta, A., Bush, R.T., Eichstaedt (Bögelein), R., Ferrio, J.P., Flanagan, L.B., Gessler, A., Martín-Gómez, P., Hirl, R.T., Kahmen, A., Keitel, C., Lai, C.-T., Munksgaard, N.C., Nelson, D.B., Ogée, J., Roden, J.S., Schnyder, H., Voelker, S.L., Wang, L., Stuart-Williams, H., Wingate, L., Yu, W., Zhao, L. and Cuntz, M.: Do ^{2}H and ^{18}O in leaf water reflect environmental drivers differently?. New Phytol, 235: 41-51, 2022. https://doi.org/10.1111/nph.18113.

Clever, H. L.: Solubility Data Series. Vol.2, Krypton-, Xenon, Radon Gas Solubilities, p. 463-468, Pergamon Press, Oxford, 1985.

Close M., Matthews M., Burbery L., Abraham P. and Scott D.: Use of radon to characterise surface water recharge to groundwater. Journal of Hydrology. 53(2): 113-127, 2014.

Costelloe, J. F., Payne, E., Woodrow, I. E., Irvine, E. C., Western, A. W., and Leaney, F. W.: Water sources accessed by arid zone riparian trees in highly saline environments, Australia. Oecologia. 156, 43-52, 2008.

Dawson, T. E. and Ehleringer, J. R.: Streamside trees that do not use stream water. Nature. 350, 335-337, 1991.

Ding, Y. L., Nie, Y. P., Chen, H. S., Wang, K. L. and Querejeta, J. I. Water uptake depth is coordinated with leaf water potential, water-use efficiency and drought vulnerability in karst vegetation. New Phytologist. 229,

1-15, 2020.

Dzikiti, S., Schachtschneider, K., Naiken, V., Gush, M., and Le Maitre, D.: Comparison of water-use by alien invasive pine trees growing in riparian and non-riparian zones in the Western Cape Province, South Africa. Forest Ecology and Management. 293, 92-102, 2013.

Ehleringer, J. R. and Dawson, T. E.: Water-uptake by plants-perspectives from stable isotope composition. Plant Cell and Environment. 15, 1073-1082, 1992.

Evaristo, J., Jasechko, S., and McDonnell, J. J.: Global separation of plant transpiration from groundwater and streamflow. Nature. 525, 91-107, 2015.

Evaristo, J., Kim, M., Haren, J. V., Pangle, L. A., Harman, C. J., Troch, P. A., and McDonnell, J. J.: Characterizing the fluxes and age distribution of soil water, Plant Water and Deep Percolation in a Model Tropical Ecosystem. Water Resources Research. 55, 3307-3327, 2019.

Fabiani, G., Schoppach, R., Penna, D. and Klaus, J. Transpiration patterns and water use strategies of beech and oak trees along a hillslope. Ecohydrology. 15(2), e2382, 2022.

Farquhar, G. D., Ehleringer, J. R., and Hubick, K. T.: Carbon isotope discrimination and photosynthesis. Annual Review of Plant Physiology and Plant Molecular Biology. 40, 503-537, 1989.

Hoehn, E. and Von Gunten, H. R.: Radon in groundwater: A tool to assess infiltration from surface waters to aquifers. Water Resources Research. 25(8), 1795-1803, 1989.

Horton, J. L. and Clark, J. L.: Water table decline alters growth and survival of *Salix gooddingii* and *Tamarix chinensis* seedlings. Forest Ecology and Management. 140, 239-247, 2001.

Jasechko, S., Seybold, H., Perrone, D., Fan, Y., and Kirchner, J. W.: Widespread potential loss of streamflow into underlying aquifers across the USA. Nature. 591, 391-395, 2021.

Li, Y., Ma, Y., Song, X. F., Wang, L. X., and Han, D. M.: A δ^2H offset correction method for quantifying root water uptake of riparian trees. Journal of Hydrology. 593, 125811, doi:10.1016/j.jhydrol.2020.125811, 2021.

Liu, B., Guan, H. D., Zhao, W. Z., Yang, Y. T., and Li, S. B.: Groundwater facilitated water-use efficiency along a gradient of groundwater depth in arid northwestern China. Agricultural and Forest Meteorology. 233, 235-241, 2017.

Long, D., Yang, W., Scanlon, B. R., Zhao, J., Liu, D., Burek, P., Pan, Y., You, L., and Wada, Y.: South-to-North

water diversion stabilizing Beijing's groundwater levels. Nature Communications. 11, 3665, doi:10.1038/s41467-020-17428-6, 2020.

Ma Y. and Song X. F.: Using stable isotopes to determine seasonal variations in water uptake of summer maize under different fertilization treatments. Science of the Total Environment. 550: 471-483, 2016.

Marek, K., Choczewski B., and Ger, R.: Iterative functional equations. Vol.32, p. 504-545, Cambridge, New York, Cambridge University Press, 1990.

Maxwell, R. M. and Condon, L. E.: Connections between groundwater flow and transpiration partitioning. Science. 353, 377-380, 2016.

Mensforth, L. J., Thorburn, P. J., Tyerman, S. D., and Walker, A. P.: Sources of water used by riparian *Eucalyptus camaldulensis* overlying highly saline groundwater. Oecologia. 100, 21-28, 1994.

Missik, J. E. C., Liu, H. P., Gao, Z. M., Huang, M. Y., Chen, X. Y., Arntzen, E., McFarland, D. P., Ren, H. Y., Titzler, P. S., Thomle, J. N., and Goldman, A.: Groundwater-river water exchange enhances growing season evapotranspiration and carbon uptake in a semiarid riparian ecosystem. Journal of Geophysical Research-Biogeosciences. 124, 99-114, 2019.

Mkunyana, Y. P., Mazvimavi, D., Dzikiti, S., and Ntshidi, Z.: A comparative assessment of water use by *Acacia longifolia* invasions occurring on hillslopes and riparian zones in the Cape Agulhas region of South Africa. Physics and Chemistry of the Earth. 112, 255-264, 2019.

Moore, G. W. and Owens, M. K.: Transpirational water loss in invaded and restored semiarid riparian forests. Restoration Ecology. 20, 346-351, 2012.

Naumburg, E., Mata-Gonzalez, R., Hunter, R. G., McLendon, T. and Martin, D. W.: Phreatophytic vegetation and groundwater fluctuations: A review of current research and application of ecosystem response modeling with an emphasis on Great Basin vegetation. Environmental Management. 35(6), 726-740, 2005.

Qian, J., Zheng, H., Wang, P. F., Liao, X. L., Wang, C., Hou, J., Ao, Y., Shen, M. M., Liu, J. J., and Li, K.: Assessing the ecohydrological separation hypothesis and seasonal variations in water use by *Ginkgo biloba L.* in a subtropical riparian area. Journal of Hydrology. 553, 486-500, 2017.

Schindler, D. W. and Donahue, W. F.: An impending water crisis in Canada's western prairie provinces. Proceedings of the National Academy of Sciences of the United States of America. 103, 7210-7216, 2006.

Schoppach, R., Chun, K. P., He, Q., Fabiani, G. and, Klaus J. Species-specific control of DBH and landscape

characteristics on tree-to-tree variability of sap velocity. Agricultural and Forest Meteorology. 307, 108533, 2021.

Smith, K., Liu, S., Hu, H. Y., Dong, X., and Wen, X.: Water and energy recovery: The future of wastewater in China. Science of The Total Environment. 637-638, 1466-1470, 2018.

Sprenger, M., Llorens, P., Cayuela, C., Gallart, F., and Latron, J.: Mechanisms of consistently disjunct soil water pools over (pore) space and time. Hydrology and Earth System Sciences. 23, 2751-2762, 2019.

Stock, B. C. and Semmens, B. X.: MixSIAR GUI User Manual, version 1.0. http://conserver.iugo-cafe.org/user/brice.semmens/MixSIAR, 2013.

Sun, S. F., Huang, J. H., Han, X. G., and Lin, G. H.: Comparisons in water relations of plants between newly formed riparian and non-riparian habitats along the bank of Three Gorges Reservoir, China. Trees. 22, 717-728, 2008.

Thorburn, P. J. and Walker, G. R.: Variations in stream water-uptake by Eucalyptus camaldulensis with differing access to stream water. Oecologia. 100, 293-301, 1994.

Wang, J., Fu, B. J., Lu, N., Wang, S., and Zhang, L.: Water use characteristics of native and exotic shrub species in the semi-arid Loess Plateau using an isotope technique. Agriculture, Ecosystems & Environment. 276, 55-63, 2019b.

Wang, J., Fu B. J., Wang, L. X., Lu N. and Li, J. Y. (2020).: Water use characteristics of the common tree species in different plantation types in the Loess Plateau of China. Agricultural and Forest Meteorology. 108020, 288-289, 2020.

Wang, P. Y., Liu, W. J., Zhang, J. L., Yang, B., Singh, A. K., Wu, J. E., and Jiang, X. J.: Seasonal and spatial variations of water use among riparian vegetation in tropical monsoon region of SW China. Ecohydrology. 12, 14, doi:10.1002/eco.2085, 2019a.

Wang, Y. S., Yin, D. C., Qi, X. F., and Xu, R. Z.: Hydrogen and oxygen isotopic characteristics of different water and indicative significance in Baiyangdian Lake. Environmental Science. 43, 4, doi:10.13227/j.hjkx.202108202, 2021. (In chinese).

White, J. C. and Smith, W. K.: Water source utilization under differing surface flow regimes in the riparian species *Liquidambar styraciflua*, in the southern Appalachian foothills, USA. Plant Ecology. 221, 1069-1082, 2020.

Winter, T. C., Harvey, J. W., Franke, O. L., and Alley, W. M.: Ground water and surface water: A single resource. Usgs U.s.geological Survey. 1139, 1998.

Xia, J. B., Ren, J. Y., Zhao, X. M., Zhao, F. J., Yang, H. J., and Liu, J. H.: Threshold effect of the groundwater depth on the photosynthetic efficiency of *Tamarix chinensis* in the Yellow River Delta. Plant and Soil. 433, 157-171, 2018.

Zaid, M. O.: A study on the convergence of variational iteration method. Mathematical and Computer Modelling. 51, 9-10, 2010. https://doi.org/10.1016/j.mcm.2009.12.034.

Zhao, D., Wang, G., Liao, F., Yang, N., Jiang, W., Guo, L., Liu, C. and Shi, Z.: Groundwater-surface water interactions derived by hydrochemical and isotopic (^{222}Rn, deuterium, oxygen-18) tracers in the Nomhon area, Qaidam Basin, NW China. Journal of Hydrology. 565, 650-661, 2018.

Zhao, L., Wang, L., Cernusak, L.A., Liu, X., Xiao, H., Zhou, M. and Zhang, S.,: Significant difference in hydrogen isotope composition between xylem and tissue water in *Populus euphratica*. Plant, Cell & Environment, 39(8), pp.1848-1857, 2016.

Zhao, L., Liu, X., Wang, N., Kong, Y., Song, Y., He, Z., Liu, Q. and Wang, L.: Contribution of recycled moisture to local precipitation in the inland Heihe River Basin. Agricultural and Forest Meteorology. 271, pp.316-335, 2019.

Zhou, T. H., Zhao, C. Y., Wu, G. L., Jiang, S. W., and Yu, Y. X., Wang, D. D.: Application of stable isotopes in analyzing the water sources of *Populus euphratica* and *Tamarix ramosissima* in the upstream of Tarim river. Journal of Desert Research. 37, 124-131, 2017. (in Chinese).

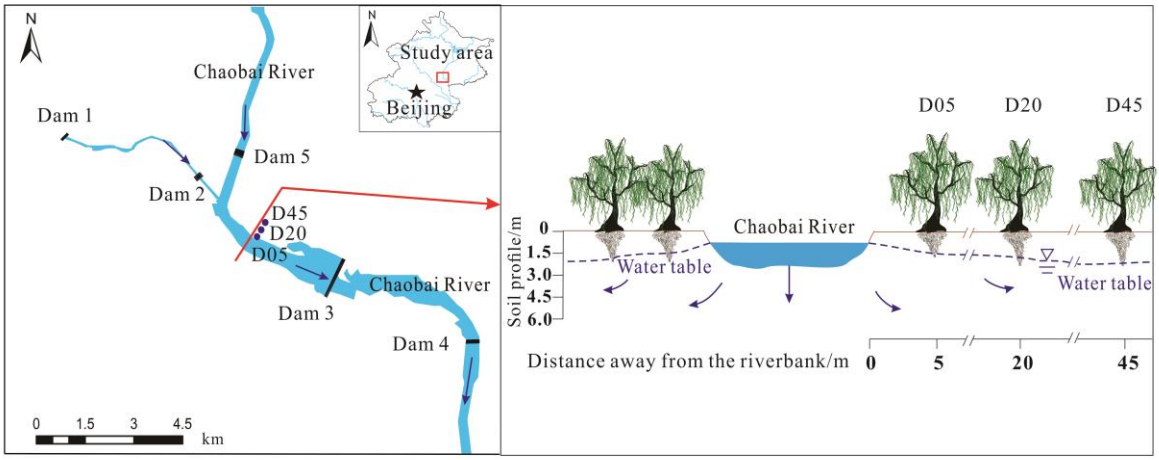

680

Figure 1: Schematic diagram of the study area and the three sampling plots (D05, D20, and D45). D05, D20, and D45 are the plots at distance of 5 m, 20 m, and 45 m away from the riverbank, respectively.

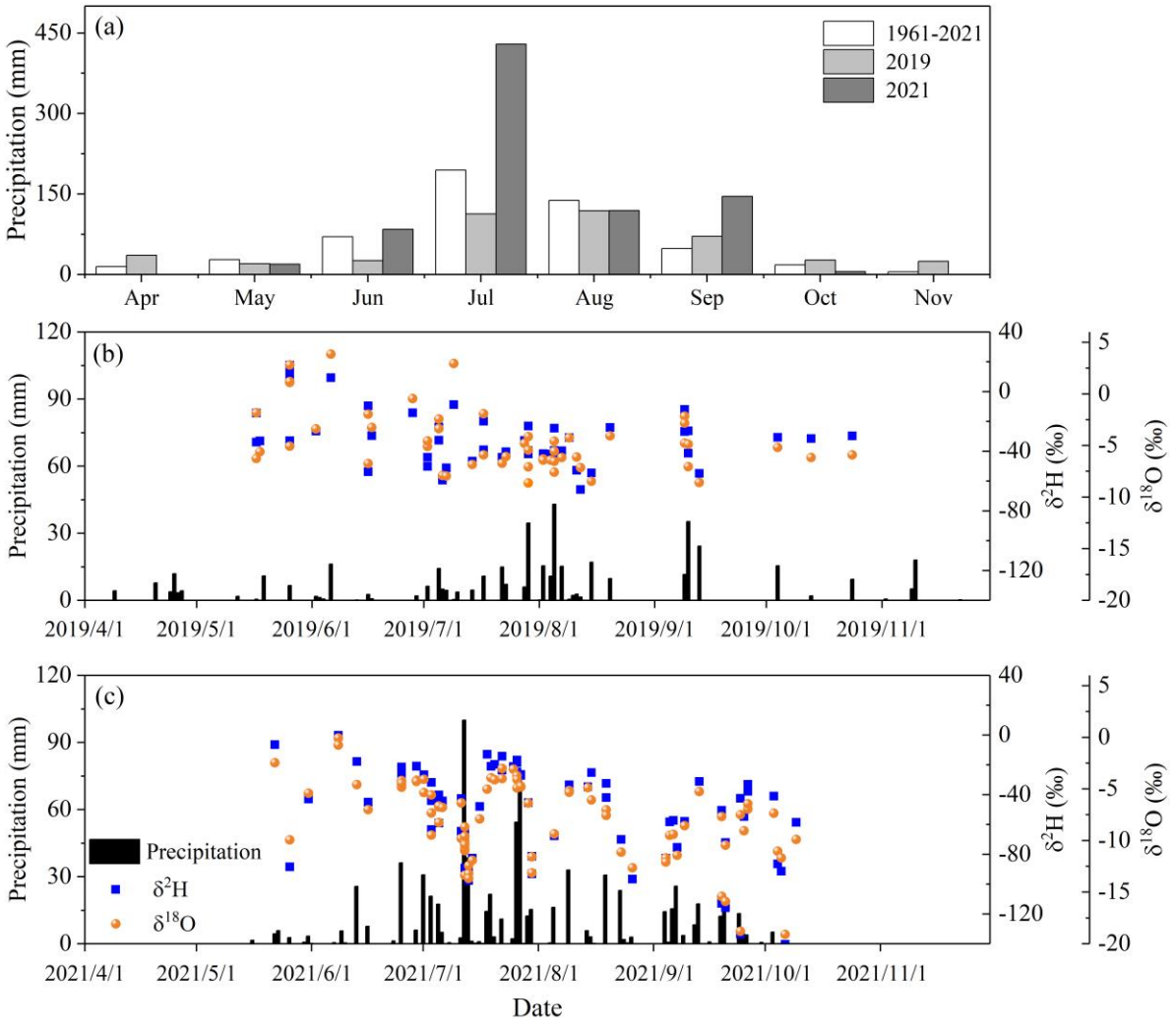

685 **Figure 2: Changes in monthly average precipitation amount from 1961 to 2021 and monthly total precipitation amount for the observation years 2019 and 2021 (a), daily precipitation amount and precipitation isotopes during 2019 (b) and 2021 (c).**

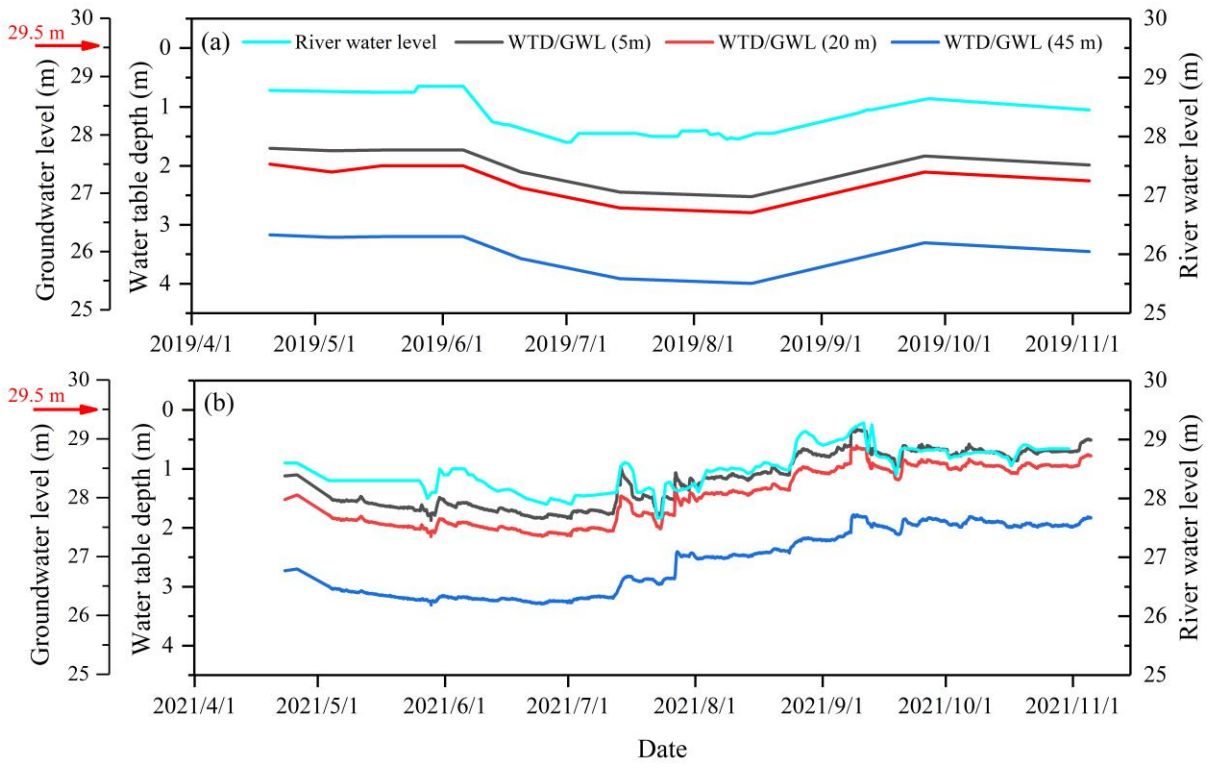

690 **Figure 3: Seasonal variations of the river water level and the water table depth (WTD)/ groundwater level (GWL) at distances of 5 m, 20 m, and 45 m away from the riverbank during the observation period in 2019 (a) and 2021 (b). The red arrow indicates the riparian ground surface level (29.5 m). The riverbed level is 26 m.**

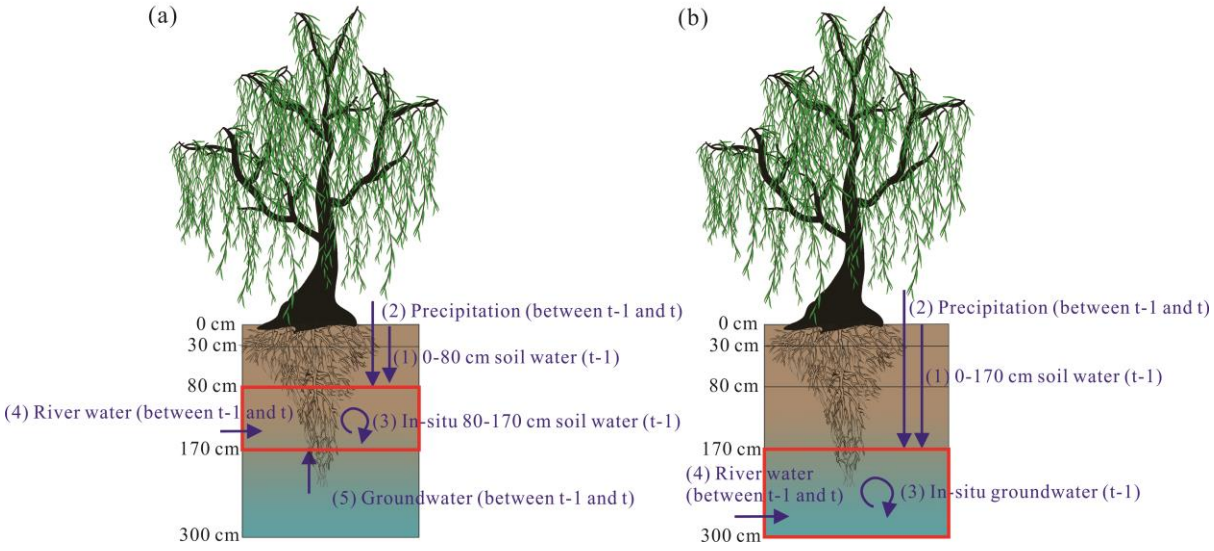

695

Figure 4: Schematic diagram for potential water sources of riparian deep soil water in the 80−170 cm layer (a) and groundwater (b).

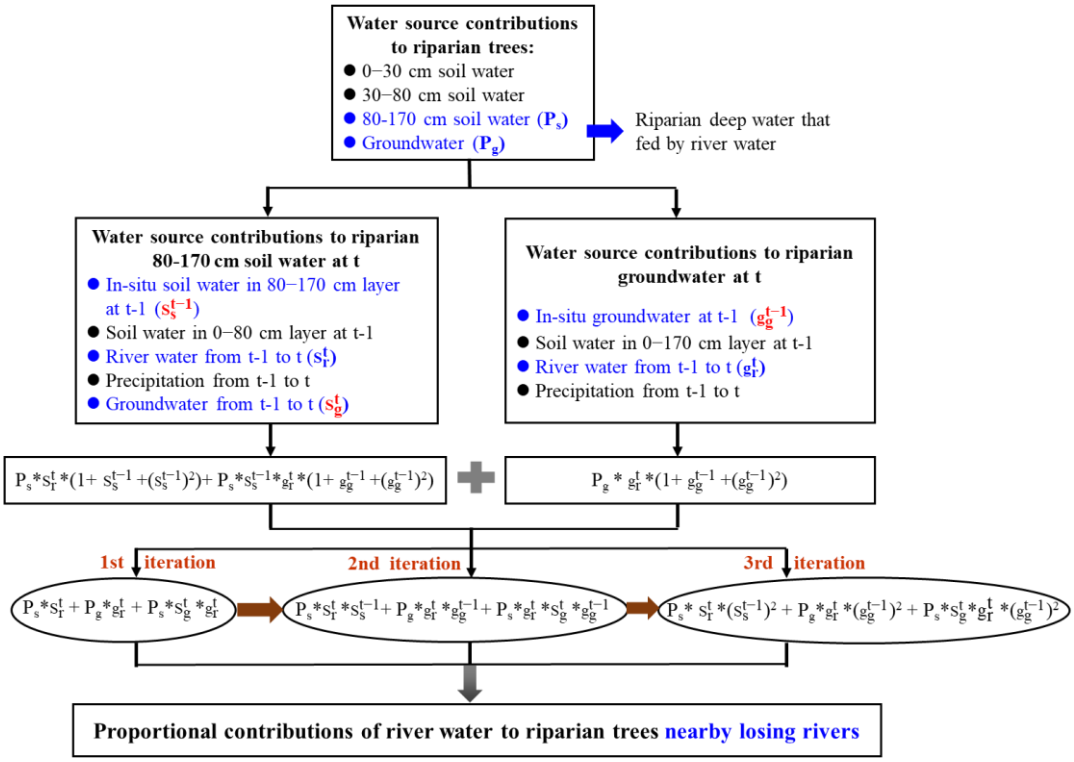

Figure 5: Flowchart for quantifying the proportional contributions of river water to riparian trees. The P_s and P_g represent the contributions of riparian deep soil water in the 80−170 cm layer and groundwater to riparian trees, respectively. The s_r^{t-1} and g_r^{t-1} represent the proportional contributions of the old river water (before t-1) to riparian deep soil water in the 80−170 cm layer and groundwater, respectively. The s_s^{t-1}, s_r^t, and s_g^t represent the proportional contributions of in-situ soil water in the 80−170 cm layer at t-1, river water during t-1 to t, and groundwater during t-1 to t for riparian deep soil water in the 80−170 cm layer at t, respectively. The g_g^{t-1} and g_r^t represent the proportional contributions of in-situ groundwater at t-1 and river water from t-1 to t for riparian groundwater at t, respectively.

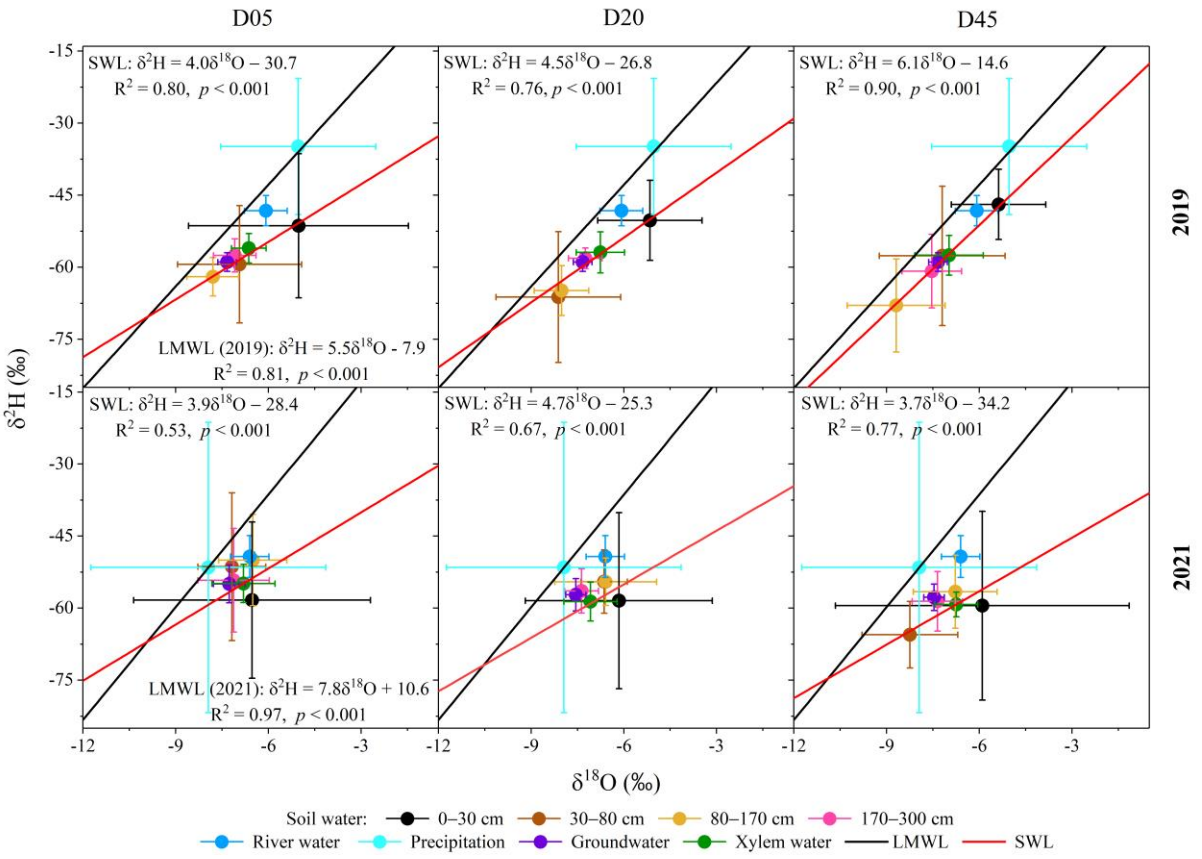

Figure 6: Dual-isotope (δ^2H and $\delta^{18}O$) biplots of different water bodies in the three plots (D05, D20, and D45) for the observation years 2019 and 2021. The local meteoric water line (LMWL) was fitted by the precipitation isotopes for each year. The soil water line (SWL) was fitted by the soil water isotopes in the four layers across three plots (D05, D20, and D45) for each year. D05, D20, and D45 are the plots at distance of 5 m, 20 m, and 45 m away from the riverbank, respectively. The error bars indicate standard deviations.

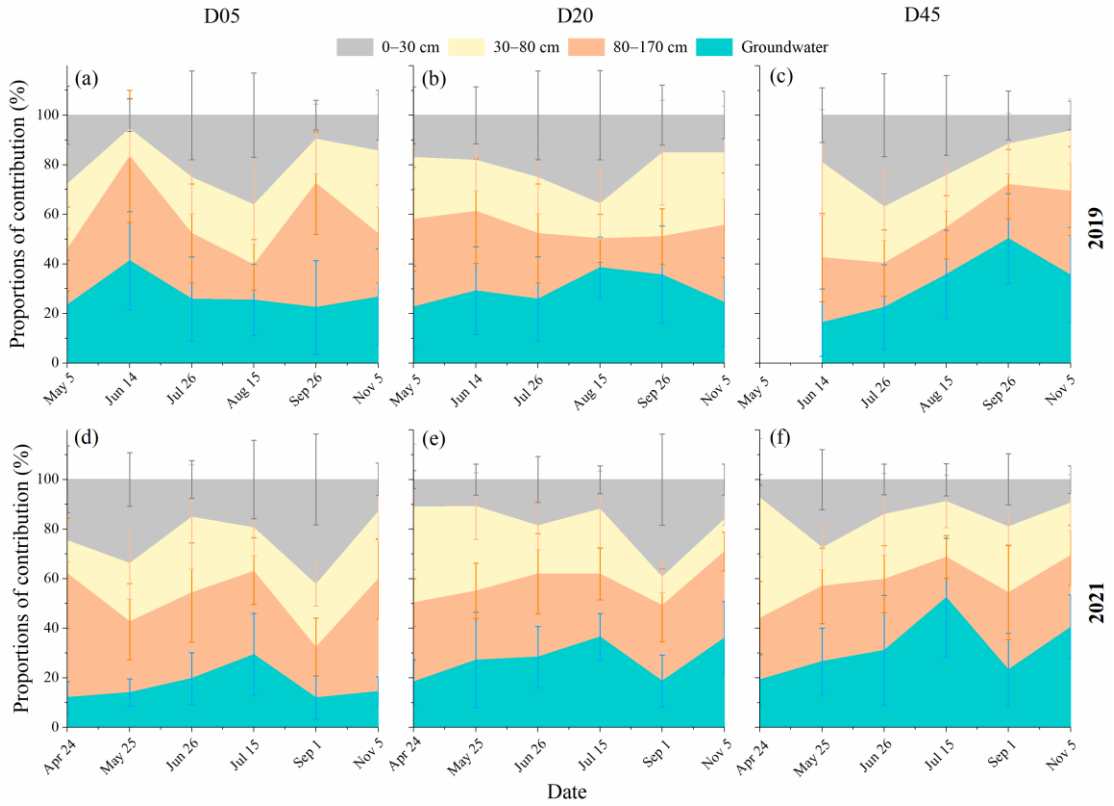

720 **Figure 7: Seasonal variations in the proportional contributions of soil water and groundwater to riparian trees in the three plots (D05, D20, and D45) for the observation years 2019 (a−c) and 2021 (d−f). D05, D20, and D45 are the plots at distance of 5 m, 20 m, and 45 m away from the riverbank, respectively. The error bars indicate standard deviations.**

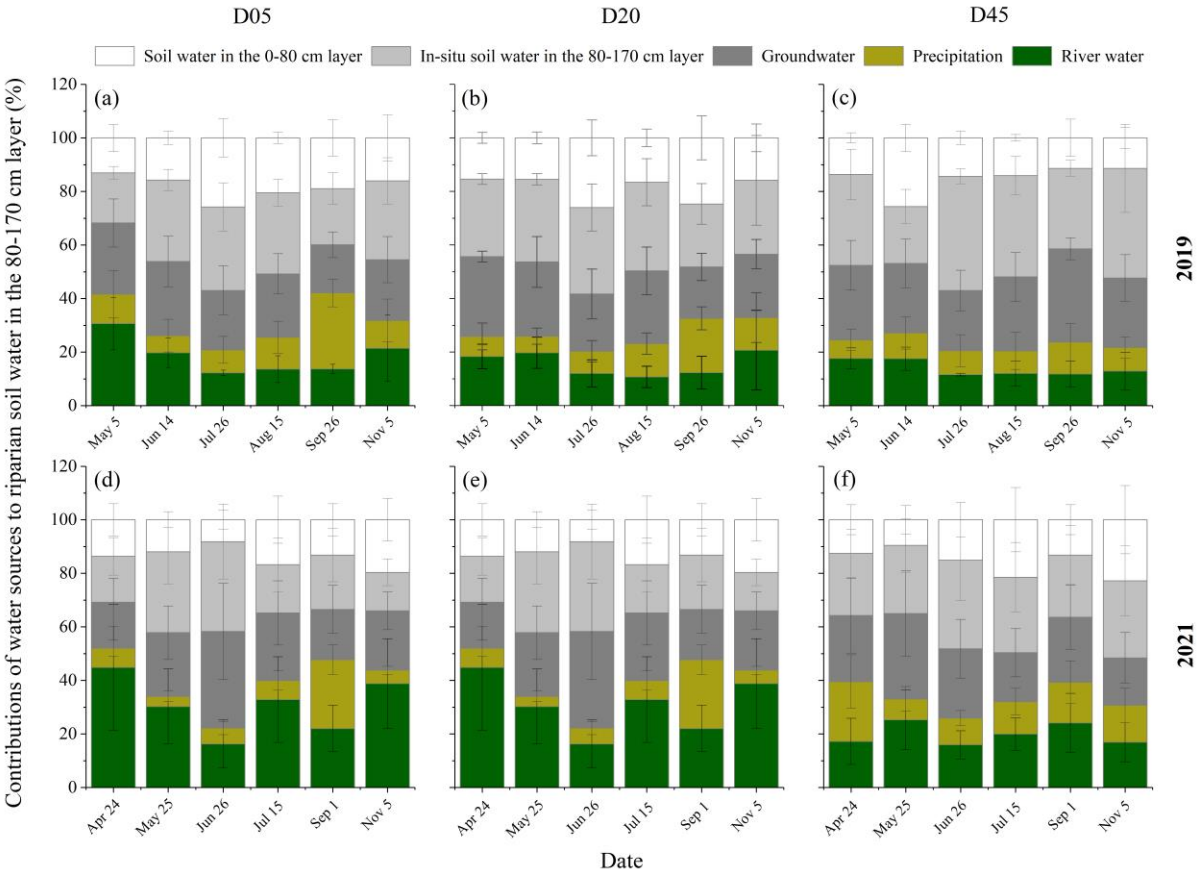

725

Figure 8: Seasonal variations in the different water source contributions to riparian deep soil water in the 80−170 cm layer in the three plots (D05, D20, and D45) for the observation years 2019 (a−c) and 2021 (d−f). D05, D20, and D45 are the plots at distance of 5 m, 20 m, and 45 m away from the riverbank, respectively. The error bars indicate standard deviations.

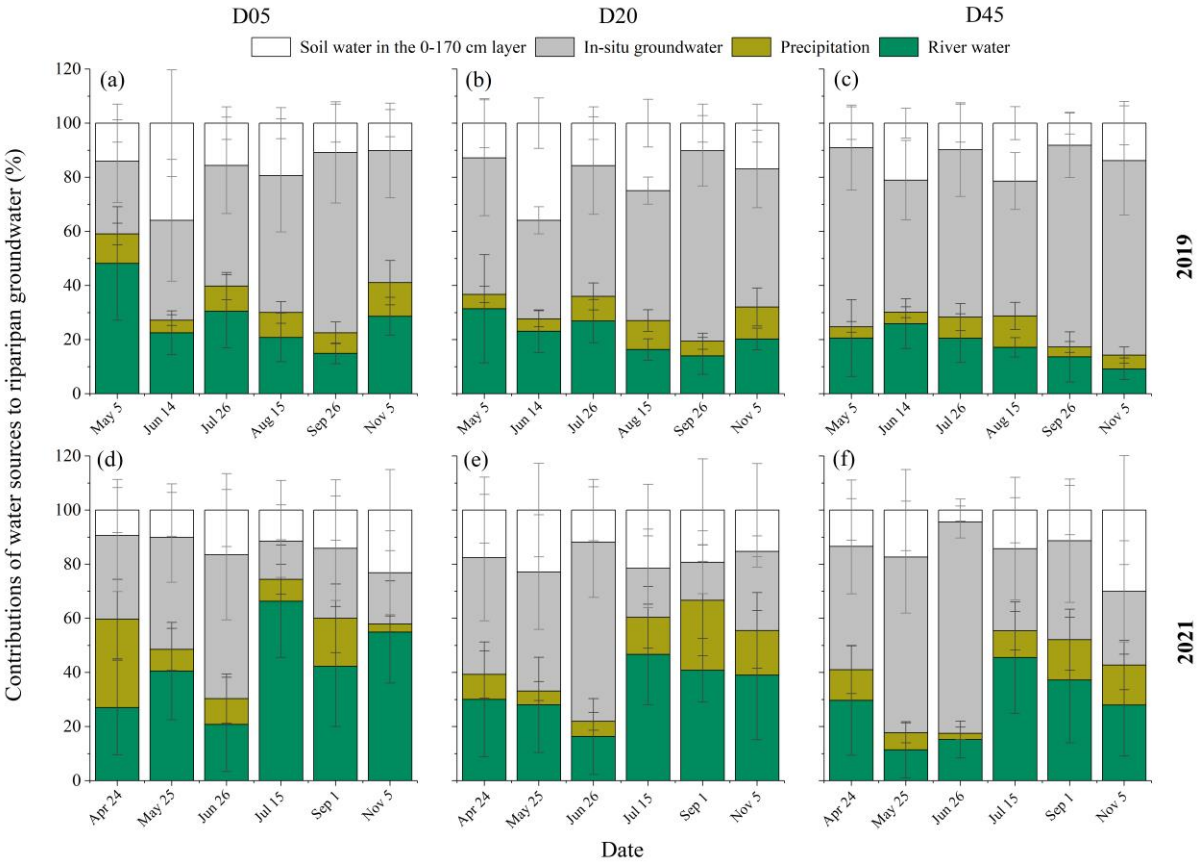

730

Figure 9: Seasonal variations in the different water source contributions to riparian groundwater in the three plots (D05, D20, and D45) for the observation years 2019 (a−c) and 2021 (d−f). D05, D20, and D45 are the plots at distance of 5 m, 20 m, and 45 m away from the riverbank, respectively. The error bars indicate standard deviations.

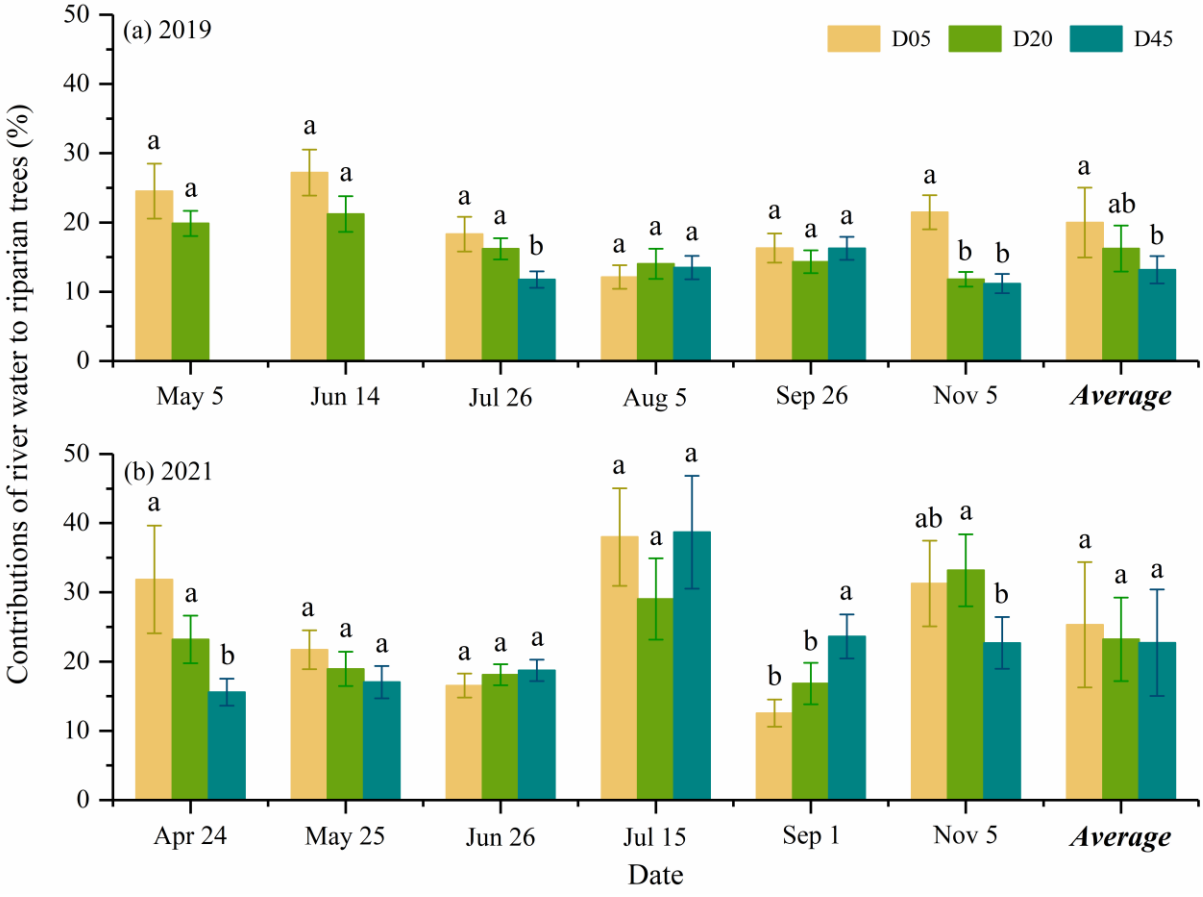

Figure 10: River water contribution (RWC) to riparian trees in the three plots (D05, D20, and D45) for each sampling campaign for the observation years 2019 (a) and 2021 (b). Different letters show a significant difference in the RWC to riparian trees between three plots for each sampling campaign ($p < 0.05$). D05, D20, and D45 are the plots at distance of 5 m, 20 m, and 45 m away from the riverbank, respectively.

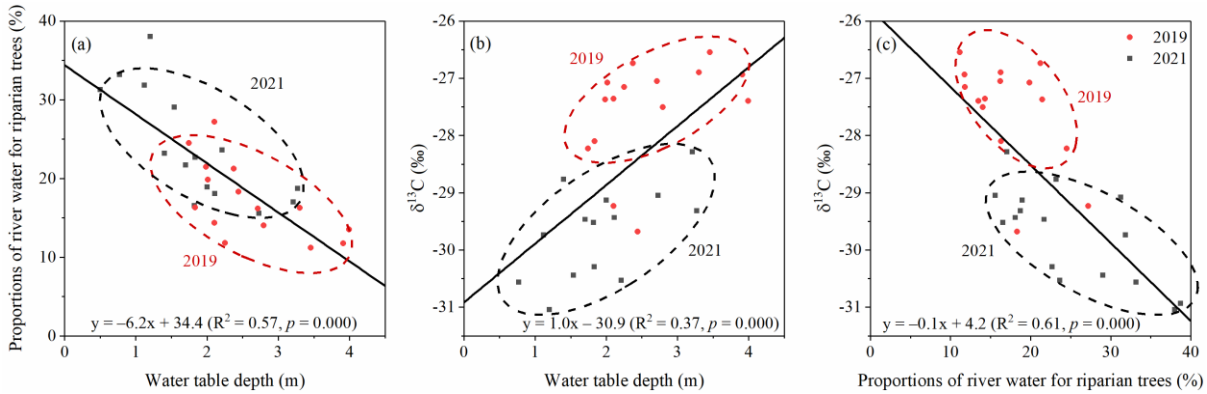

Figure 11: Relationships between the proportions of river water contributions for riparian trees and the water table depth (a), between the leaf $\delta^{13}C$ values and the water table depth (b), and between the leaf $\delta^{13}C$ values and proportions of river water contributions for riparian trees (c).

Table 1: The ^{222}Rn values in river water, background groundwater and riparian groundwater in three plots (D05, D20, and D45), and the average residence time of recharged groundwater from river water (T_{res}, day) in 2021. The background groundwater represents groundwater in aquifers more than 100 m away from the riverbank.

	River water	Background groundwater	Riparian groundwater		
			D05	D20	D45
^{222}Rn value (Bq/m^3)	610.1 ± 212.3	7400 ± 35.4	610.1 ± 107.5	763.3 ± 118.3	787.4 ± 153.2
T_{res} (days)	0	Null	0	0.13 ± 0.1	0.15 ± 0.13

Notes: D05, D20, and D45 are the plots at distance of 5 m, 20 m, and 45 m away from the riverbank, respectively.

Table 2: Leaf $\delta^{13}C$ values of riparian *S. babylonica* in the three plots (D05, D20, and D45) during the observation period in 2019 and 2021.

	Leaf $\delta^{13}C$ value (‰)							
	2019							
	May 5	Jun 14	Jul 26	Aug 15	Sep 26	Nov 5	Mean	STD
D05	−28.8	−29.2	−29.7	−30.4	−28.1	−27.4	−28.8	1.0
D20	−27.1	−26.7	−27.1	−27.5	−27.4	−27.2	−27.1	0.2
D45	Null	−27.2	−26.9	−27.4	−26.9	−26.5	−27.0	0.3
	2021							
	Apr 24	May 25	Jun 26	Jul 14	Sep 1	Nov 5	Mean	STD
D05	−29.7	−29.5	−29.5	−31.0	−29.5	−29.1	−29.7	0.6
D20	−28.8	−29.1	−29.4	−30.4	−30.1	−30.3	−29.7	0.7
D45	−29.0	−29.0	−29.4	−30.8	−30.1	−30.0	−29.7	0.9

Note: D05, D20, and D45 are the plots at distance of 5 m, 20 m, and 45 m away from the riverbank, respectively. STD represents standard deviations.